Ocean Engng, Vol. 18, No 3, pp. 225–250, 1991.
Printed in Great Britain.

0029–8018/91 $3.00 + .00
Pergamon Press plc

CHAOTIC BEHAVIOR AND STABILITY OF FREE-STANDING OFFSHORE EQUIPMENT

SOLOMON C. S. YIM and HUAN LIN
Ocean Engineering Program, Department of Civil Engineering, Oregon State University, Corvallis, OR 97331, U.S.A.

Abstract—The rocking behaviour and overturning stability of free-standing offshore equipment subjected to support excitations is investigated. This study focuses on systems with realistic slenderness ratios subjected to *both* horizontal and vertical excitations. Fully nonlinear equations governing the rocking motion are used in the analysis. Additional nonlinear effects due to the transition of governing equations at impact, the abrupt reduction in angular velocity associated with impact energy dissipation, and the coupling of the vertical (parametric) excitation with the rocking response are examined in detail. Analytical methods and numerical techniques are developed to determine the response time histories, phase diagrams, Poincaré maps, Lyapunov exponents, and fractal dimensions. *Chaotic* and *quasi-periodic* responses are shown to co-exist with *periodic* and *overturning* responses. Results show that the response of non-slender (fully nonlinear) systems are more sensitive to perturbations in system and excitation parameters than their slender (piecewise-linear) counterparts. The transition nonlinearity at impact induces chaotic behavior, and is the major cause of response sensitivity. Increasing the impact energy dissipation decreases the sensitivity of the rocking response. For the range of magnitude considered, increasing vertical excitation increases the sensitivity of the rocking response.

NOMENCLATURE

a_{gx}	horizontal ground acceleration
a_{gy}	vertical ground acceleration
a_x	amplitude of horizontal excitation
a_y	amplitude of vertical excitation
A_x	normalized amplitude of horizontal excitation, $A_x = a_x/(g\theta_{cr})$
A_y	normalized amplitude of horizontal excitation, $A_y = a_y/g$
B	width of block
d_c	fractal dimension
e	coefficient of restitution
g	acceleration of gravity
H	height of block
I_o	mass moment of inertia
M	mass of object
r_a	ratio of vertical vs horizontal excitation amplitude; $r_a = a_y/a_x$
r_f	ratio of vertical vs horizontal excitation frequency; $r_f = \omega_y/\omega_x$
R	radius of rotation
S^3	three-dimensional trajectory space
S^2	two-dimensional phase space
T_x	period of horizontal excitation
W	weight of object
θ	rotation angle of rocking block
θ_{cr}	critical angle
$\dot{\theta}$	angular velocity
Θ	normalized angle, $\Theta = \theta/\theta_{cr}$

$\dot{\Theta}$ normalized angular velocity, $\dot{\Theta} = \dot{\theta}/\theta_r$,
λ Lyapunov exponent
ω_x frequency of horizontal excitation
ω_y frequency of vertical excitation.

1. INTRODUCTION

MANY OFFSHORE surveillance, exploration, drilling and operational equipment on board ships and floating production systems are not firmly anchored to their supporting base. Some, in fact, may be considered to be free-standing. These free-standing items of equipment, which are regarded as rigid objects in this study, may sometimes be set into rocking motion due to the motion of the supporting structure induced by wind, wave and current loads (Fig. 1). Overturning of these items of equipment can be costly and may threaten the safety of nearby workers. Thus an understanding of the rocking behavior and overturning stability of free-standing objects subjected to base excitations is essential for developing safe offshore operation guidelines, preserving existing equipment, and improving analysis and design procedures for new equipment.

The rocking behavior and overturning stability of rigid objects has long been of interest to engineers [see Ishiyama (1982) for an excellent literature review]. Although the behavior of the rocking motion is very complex, limited by the state of technology at the time, earlier stability studies took a simplistic approach and concentrated on developing an equivalent lateral design force to take into account the dynamic effects of rocking motion [Ishiyama (1982)].

With the advances in analysis and experimental techniques, significant progress has been made recently in identifying the unique features of the dynamic rocking behavior. From the 1960s to the early 1980s, researchers were interested in the dynamic rocking response of free-standing objects to earthquake excitations. Housner (1963) performed a probabilistic analysis of the rocking response to simplified earthquake (white-noise)

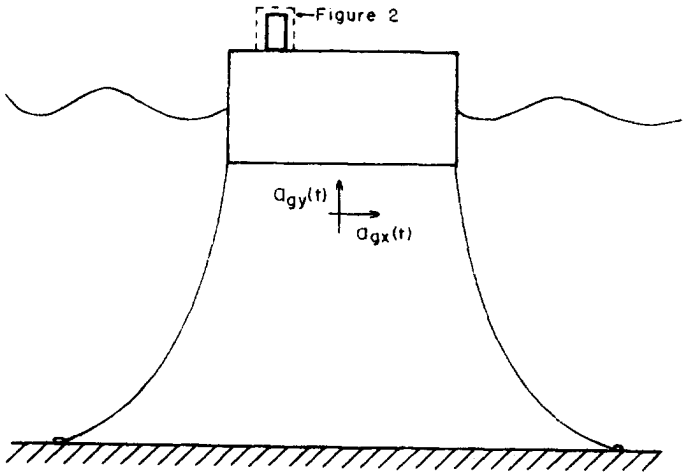

FIG. 1. Free-standing equipment on board a compliant offshore structure

excitations. He pointed out that the stability of slender objects subjected to random ground motion is much greater than would be inferred from its stability against an equivalent static horizontal force proposed in earlier studies. Aslam *et al.* (1980) conducted a series of experiments on the Berkeley shaking table and found that the rocking response could be extremely sensitive to system parameters and the detail of the ground excitations. In fact, for some combinations of system parameters, the responses were so sensitive that the experiments were deemed unrepeatable. Yim *et al.* (1980) examined the sensitivity of the rocking response in a statistical sense, and conducted a numerical study to identify the parametric dependency of overturning stability on system parameters and excitation intensity. Their results confirmed that the rocking response is very sensitive to small changes in system parameters as well as the detail of excitations, and that statistical trends can only be established with a large sample size.

Recognizing the severe complexity of the rocking response and averting the randomness in the excitations, researchers since the mid-1980s have been concentrating on "simplified" rocking systems subjected to simple forms of deterministic excitations. Spanos and Koh (1984) and Tso and Wong (1989) examined the stability of *slender* objects subjected to horizontal *simple harmonic* ground excitation. Using a piecewise-linear model they determined the rocking stability of objects and identified safe and overturning regions in an amplitude–frequency plane. In addition to harmonic responses, steady-state (bounded) subharmonic responses were detected. Analytical procedures were developed for determining the amplitudes of the predominant modes.

These recent studies have provided valuable insights into the behavior of slender rocking objects. However, there are severe limitations on the applicability of their results in the ocean engineering area. Although the analyses of simplified systems [Housner (1963), Spanos and Koh (1984) and Tso and Wong (1989)] might be suitable for some types of land-based structures, they are in general not adequate for modeling the rocking behavior of free-standing offshore equipment. Because the individual equations of motion in the simplified systems were linearized, in order for their analyses to apply, the rocking objects might have to be unrealistically slender (i.e. very large slenderness ratios). On the contrary, the slenderness ratios of offshore equipment are in general not large and the effects of geometric nonlinearity may have to be taken into account. In addition, the analytical methods developed from the simplified piecewise-linear theory could not take into account the effects of vertical excitation, which induces nonlinear coupling between rocking response and the (parametric) excitation. The vertical motion of floating offshore structures such as ships, moored barges and tension-leg platforms normally cannot be neglected. The combination of horizontal and vertical excitations at different frequencies (combination tones) may induce responses that are significantly different from a single frequency excitation (Nayfeh and Mook, 1979). Recently, in an experimental study, Wong and Tso (1989) examined the rocking response to horizontal harmonic excitations and found that there were responses that could not be accounted for by the analytical methods developed by Spanos and Koh (1984) and Tso and Wong (1989).

The fully nonlinear studies by Yim *et al.* (1980) and Aslam *et al.* (1980) were restricted to statistical behavior of rocking response to earthquake-type transient random excitations. Their results cannot be directly extended to steady-state response to deterministic excitations.

The objective of this investigation is to examine the major causes of sensitivity of the rocking response behavior via simple deterministic excitations and to identify and resolve the unknown responses found in Wong and Tso's experimental study. The influence of the nonlinear effects, especially the geometric nonlinearity caused by finite slenderness ratio and the presence of vertical (parametric) excitation, on the sensitivity will be studied in detail using recently developed analytical and numerical techniques.

2. SYSTEM MODEL

2.1. *Equations of motion*

The free-standing offshore equipment is modeled as a rectangular rigid object subjected to horizontal and vertical base motion excitations (Fig. 2). In Yim *et al.* (1980), the governing equations of motion for the rocking object subjected to horizontal and vertical base excitations, taking into account all nonlinear effects, were derived. A brief summary of the derivation is presented here.

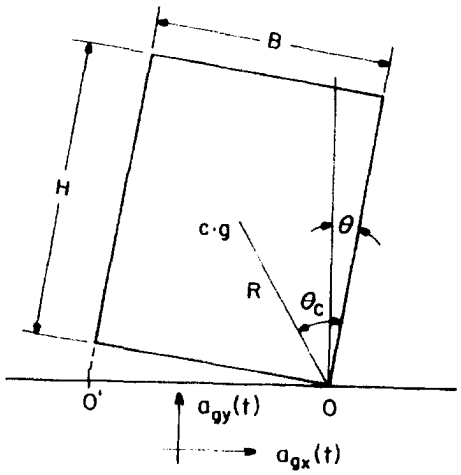

FIG. 2. Idealization of free-standing equipment as a rigid rocking object, subjected to horizontal and vertical excitations.

2.1.1. *Initiation of rocking.* Assuming the coefficient of friction is sufficiently large so that there will be no sliding between the object and the base, depending on the support accelerations, the object may move rigidly with the base or be set into rocking about the centers of rotation O and O'. When subjected to base accelerations in the horizontal and vertical directions, the object will be set into rocking when the overturning moment of the horizontal inertia force about one edge exceeds the restoring moment due to the weight and the vertical acceleration of the object:

$$\frac{Wa_{gx}H}{2g} > \left(W + \frac{Wa_{gy}}{g}\right)\frac{B}{2} \tag{1a}$$

or

$$a_{gx} > \frac{Bg}{H}\left(1 + \frac{a_{gy}}{g}\right) \tag{1b}$$

where W is the weight of the object, H and B are the height and width of the object, g is acceleration of gravity, and a_{gx} and a_{gy} are the horizontal and vertical foundation accelerations, respectively. The geometric and gravity centers of the object are assumed to coincide.

2.1.2. *Governing equations.* The governing equation of motion for the rigid object with positive angular rotation can be derived by taking moments about corner O:

$$I_o\ddot{\theta} + MRa_{gx}\cos(\theta_{cr}-\theta) + M(g+a_{gy})R\sin(\theta_{cr}-\theta) = 0 \tag{2a}$$

where

I_o = moment of inertia of the block about O;
M = W/g, the mass of the block;
and R = the distance from O to the center of mass of the block.

$\theta_{cr} = \cot^{-1}(H/B)$ is the critical angle beyond which overturning will occur for the object under gravity alone. Similarly, the rocking about O' is governed by the equation:

$$I_o\ddot{\theta} + MRa_{gx}\cos(\theta_{cr}+\theta) - M(g+a_{gy})R\sin(\theta_{cr}+\theta) = 0. \tag{2b}$$

2.1.3. *Impact energy dissipation.* Impact occurs when the angular rotation crosses zero approaching from either positive or negative and the base surfaces recontact. Associated with the impact is a transition from rocking about one corner to rocking about the other and a finite amount of energy loss, which can be accounted for by reducing the angular velocity of the object after impact. As in Yim *et al.* (1980), the energy dissipation is represented by an impact parameter e and has the following relationship

$$\dot{\theta}(t^+) = e\dot{\theta}(t^-) \tag{3}$$

where e = the coefficient of restitution; t^+ = the time just after impact; and t^- = the time just before impact.

2.1.4. *Base excitations.* As in Spanos and Koh (1984) and Tso and Wong (1989), the horizontal base acceleration is assumed to be harmonic with constant amplitude and frequency, i.e.

$$a_{gx} = a_x\cos\omega_x t. \tag{4a}$$

To examine the influence of vertical excitation, the vertical base acceleration is also assumed to be simple harmonic in this study, but with a different amplitude and frequency to those of the horizontal component:

$$a_{gy} = a_y \cos\omega_y t. \tag{4b}$$

2.2. *Sources of nonlinearity*

There are four sources of nonlinearity in the governing equations [Equations (2a) and (2b)] of dynamic response of the *fully nonlinear* free-standing rocking object: (1) the transition from one governing equation to the other at impact when the center of rotation changes from one edge to the other; (2) the impact energy dissipation which induces a jump discontinuity (an abrupt reduction) in an angular velocity; (3) the geometric effect of finite slenderness ratio of the object; and (4) the coupling of the vertical excitation with the rocking response. These nonlinearities are examined in detail in later sections. The effects of each individual nonlinearity are sequentially isolated when possible.

2.3. *Analysis procedure*

Because the system considered is nonlinear and rather complex, no analytical solutions have been found for the response of the general system governed by Equations (2a) and (2b). In this study, the response to base excitations is obtained by numerically integrating the governing equations. The procedure employed is similar to that of Yim *et al.* (1980). The condition for initiation of rocking is described by Equation (1). When motion is initiated, the sign of the ground acceleration a_{gx} determines whether the equation for positive or negative rotation is to be used for the next time step. The equation for positive angular rotation is employed for positive a_{gx} and the equation for negative rotation is used for negative a_{gx}. The same equation is used for subsequent time steps. The time steps are constant except when the sign of rotation θ changes. When such a change occurs, such as during time step t_j to t_{j+1}, this time step is divided into two parts. Using the equation of motion valid at t_j, the exact time t^*, $t_j < t_{j+1}$, at which θ becomes zero is determined by an implicit iterative procedure. Just before impact $\theta(t^-) = 0$ and velocity is $\dot{\theta}(t^-)$. The energy loss due to impact is governed by the coefficient of restitution e. Immediately after impact $\theta(t^+) = 0$ and $\dot{\theta}(t^+) = e\dot{\theta}(t^-)$. With these initial conditions, the equation of motion valid for conditions at $t = t^*$ immediately after impact is solved over the time interval t^* to t_{j+1} and subsequent time intervals until the rotation angle θ again changes sign. The above-mentioned process is then repeated. With the time step division at transition, the numerical procedure remains consistent with the physical behavior at all times and the constant integration time step is maintained. The numerical solution procedure was implemented in a computer program using a fourth-order Runge–Kutta integration method.

3. TYPES OF RESPONSES

The responses of the fully nonlinear rocking objects subjected to horizontal and vertical harmonic base excitations can be categorized into four types. The characteristics of these responses are described in this section. The mathematical relationships among the three bounded responses will be discussed later when the Poincaré map is introduced.

When subjected to harmonic base excitations, for a given combination of fixed excitation frequencies, if the corresponding excitation amplitudes are too large, the response of a free-standing object may become *unbounded*, leading to *overturning* of

the object after a finite amount of time. On the other hand, if the excitation amplitudes are sufficiently large to induce rocking but not too large to cause overturning, the response will eventually settle into a *bounded* motion. Based on classical nonlinear analysis, it was believed that, under periodic excitations, all bounded responses were *periodic*. Thus, past studies of bounded responses had been concentrated on periodic motions [Spanos and Koh (1984) and Tso and Wong (1989)]. It will be shown in later sections that there exist two additional types of bounded responses, namely *quasi-periodic* and *chaotic* responses.

For convenience of plotting and interpreting numerical results, it is useful to normalize the angular displacement and velocity responses by the critical angle as follows:

$$\Theta = \theta/\theta_{cr} \tag{5a}$$

$$\dot{\Theta} = \dot{\theta}/\theta_{cr}. \tag{5b}$$

These normalized variables are used in all displays of the computed responses.

3.1. *Overturning response*

For some combinations of excitation amplitudes and frequencies the magnitudes of the rocking response, starting from quiescent conditions after a finite time period, do not return to zero but increase without bound with time, i.e.

$$\lim_{t\to\infty} |\theta(t)| \to \infty. \tag{6}$$

Physically, these types of responses lead to overturning when the magnitude of the angular rotation far exceeds the critical angle. Typically, for fixed system parameters, overturning responses are associated with large excitation amplitudes. The time history and phase diagram of a typical example of an overturning response are shown in Fig. 3a and b, respectively. Overturning responses are undesirable and their occurrence should be avoided.

3.2. *Periodic response*

A steady-state bounded response of a dynamical system is called periodic if the motion repeats itself with a fixed time T, i.e.

$$x(t+T) = x(t) \tag{7}$$

for all time t. The minimal T which satisfies this condition is called the period of the motion. It is well known that for linear systems, the period of a steady-state bounded response is equal to that of the excitation. In other words, the response is harmonic, or primary resonance. However, for nonlinear systems, in addition to the primary resonance response, subharmonic, superharmonic and sub-superharmonic (where the response period is equal to an integer multiple, an integer fraction, and a rational fraction of the excitation period, respectively) are also possible [Nayfeh and Mook (1979)]. For the range of excitations considered in this study, harmonic and subharmonic rocking responses are found to occur frequently. The time history and phase diagram of a typical example of a one-third subharmonic response are shown in Fig. 4a and b, respectively.

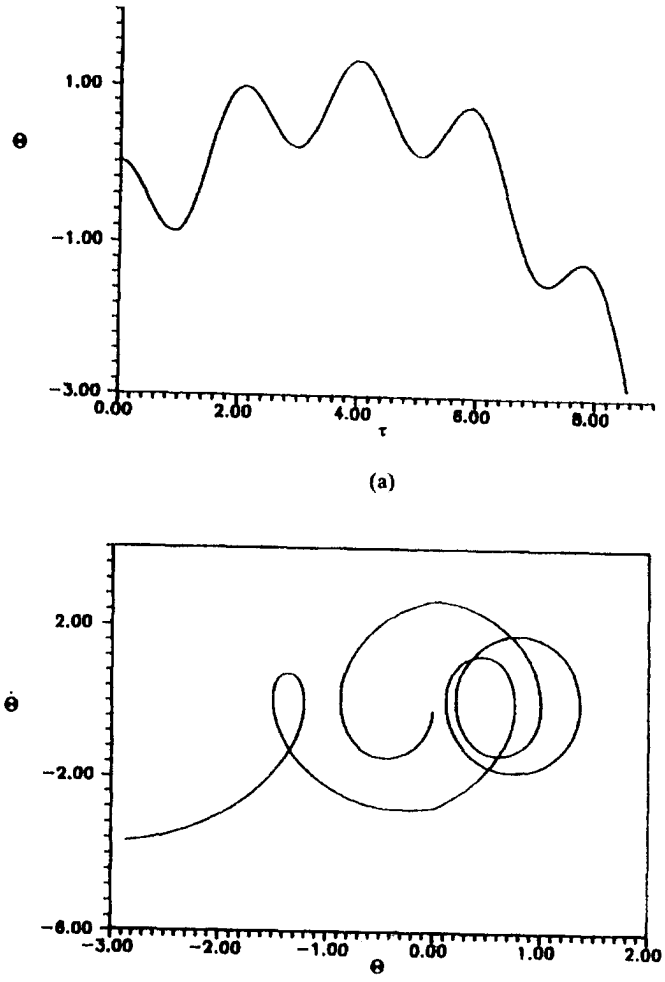

FIG. 3. Overturning response: (a) time history and (b) phase diagram; $A_1 = 1.75$, $T_1 = 2.0$ and $e = 0.925$.

As discussed in detail in Spanos and Koh (1984), periodic responses are stable. If a small perturbation in the initial conditions is introduced, the rocking response will eventually converge to the periodic motion corresponding to the particular system and excitation parameters. Thus periodic responses are stable, i.e. insensitive to small changes in initial conditions. In addition, the stability boundaries of periodic responses are continuously dependent on systems parameters, and it can be shown that except at the boundary (which are rare occurrences), periodic responses are also stable with respect to perturbations in system parameters. Hence, in general, in regions of system and excitation parameters where periodic responses occur, the response behavior is stable and insensitive to small changes in system and excitation parameters.

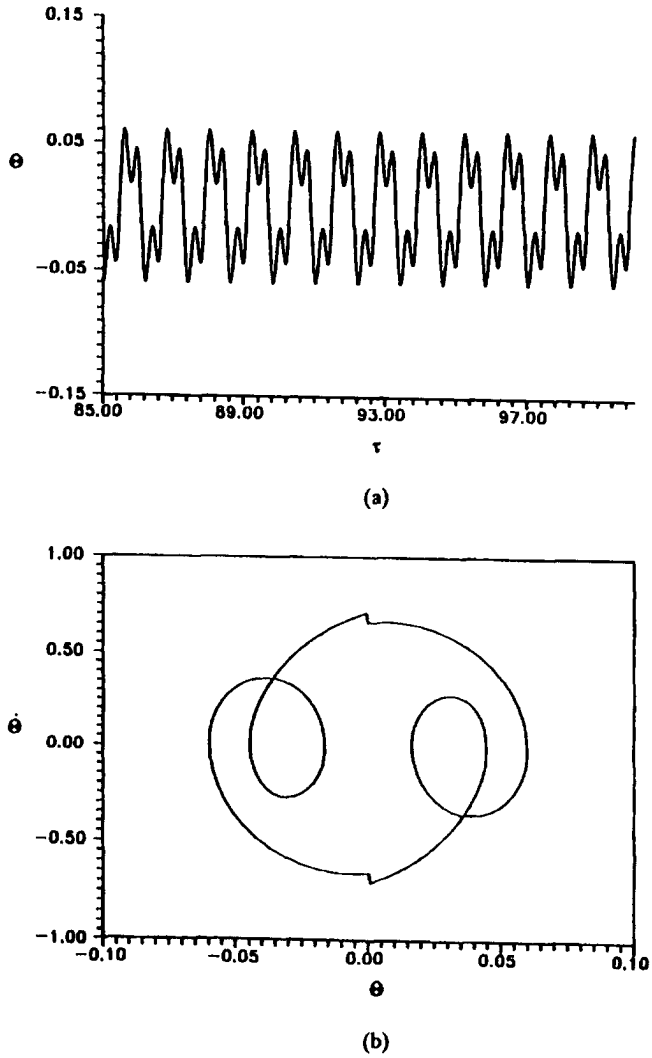

FIG. 4. Periodic response: (a) time history and (b) phase diagram; $A_v = 6.5$, $T_v = 0.4$ and $e = 0.925$.

3.3. *Quasi-periodic response*

A new type of rocking response discovered in this study is the quasi-periodic motion, which is a combination oscillation consisting of two or more incommensurate frequencies (Moon, 1987). The simplest type of combination oscillation takes the form

$$X(t) = b_1\cos(\omega_1 t + d_1) + b_2\cos(\omega_2 t + d_2) \tag{8}$$

where ω_1 and ω_2 are incommensurate, i.e. ω_1/ω_2 is an irrational number, and d_1 and d_2 are appropriate phase shifts. In this case, a periodic motion is modulated in some way by a second motion, which is periodic but with a different period. The time history

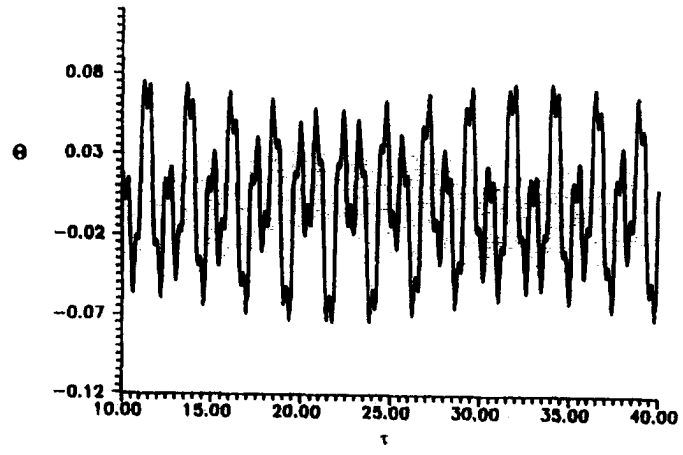

(a)

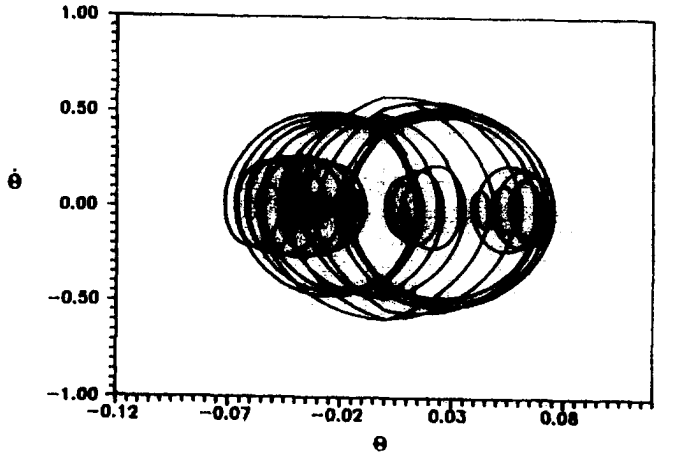

(b)

FIG. 5. Quasi-periodic response: (a) time history and (b) phase diagram; $A_1 = 4.0$, $T_1 = 0.4$ and $e = 1.0$.

and phase diagram of a typical example of a quasi-periodic response are shown in Fig. 5a and b, respectively.

Quasi-periodic responses are relatively rare in general and only occur under ideal conditions (e.g. undamped systems). Their occurrence usually indicates a transition of the responses of the system between stable periodic motions and "unstable" chaotic motions (Thompson and Stewart, 1986).

3.4. *Chaotic response*

A second new type of rocking response discovered in this study is chaotic motion. Its behavior is characterized by a random-like, unpredictable aspect as well as a certain

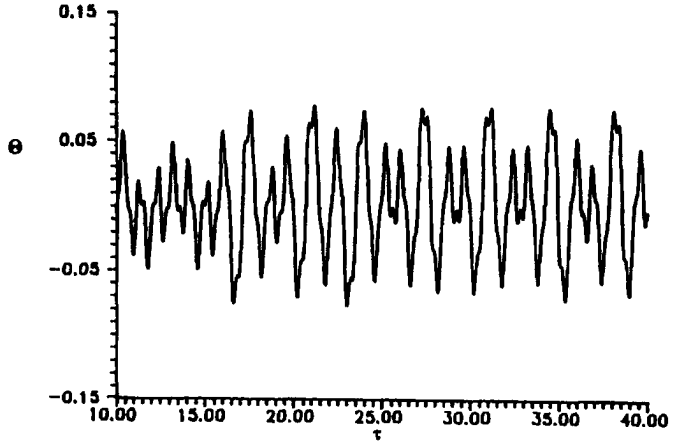

(a)

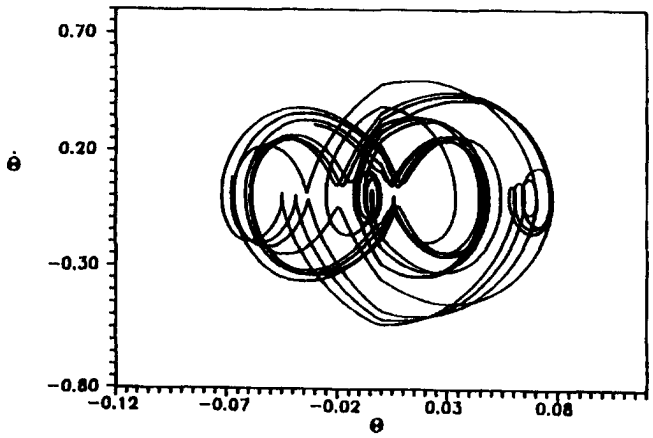

(b)

FIG. 6. Chaotic response: (a) time history and (b) phase diagrams; $A_x = 3.0$, $T_x = 0.4$ and $e = 1.0$.

order in the motion, although the excitation is straightly deterministic and periodic (Thompson and Stewart, 1986). The unpredictability arises from its *sensitive dependence on initial conditions* (Moon, 1987). Chaotic motion for which trajectories with seemingly infinitesimal different initial conditions diverge exponentially leads to large differences in long-term predictions of the response. The time history and phase diagram of a typical example of a chaotic response are shown in Fig. 6a and b, respectively.

The sensitivity of a chaotic response is demonstrated in Fig. 7, which shows the rocking responses of two identical systems with an infinitesimal difference in initial displacement. Note that, as expected, the two chaotic responses having initial conditions with no perceptible differences diverge rapidly with time.

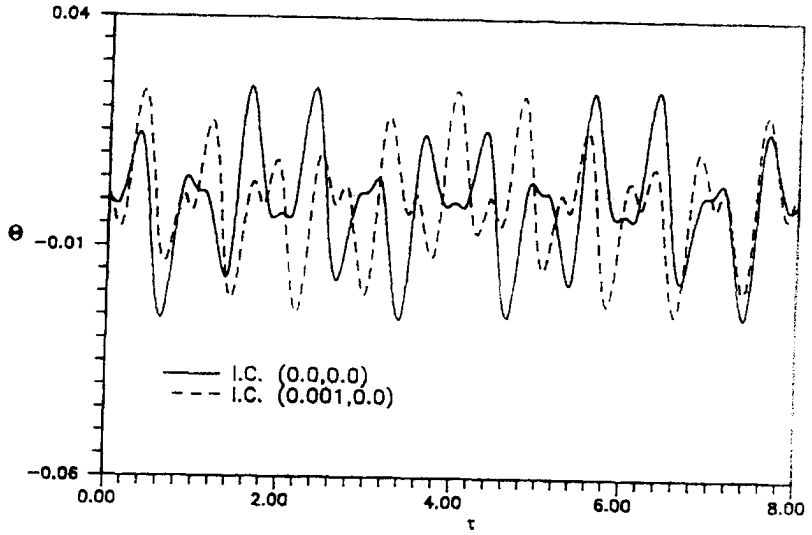

FIG. 7. Sensitivity to initial condition of chaotic response; $A_1 = 3.0$, $T_1 = 0.4$ and $\zeta = 1.0$.

Systems with parameters for which chaotic response occur may be considered unstable, i.e. sensitive to the combination of frequencies and amplitudes of the excitations. It should be noted that sensitivity of the response is excitation-dependent. For the same given system, its response may be overturning, periodic, quasi-periodic or chaotic, depending on the frequency and amplitude parameters of the excitation.

4. POINCARÉ MAPS AND VERIFICATION TECHNIQUES

Based on the physical description of the four types of responses discussed above, overturning responses can be readily identified by inspection of their time histories and phase diagrams. However, in general, the difference between periodic response with a long period, quasi-periodic and chaotic responses may not be obvious from the time histories and phase diagrams. To clarify the relationships among the three types of bounded responses, their formal mathematical definitions are presented via the Poincaré map. Techniques to identify and differentiate the three types of responses are also introduced.

4.1. *Poincaré maps*

The solution curve of the rocking response [governed by Equation (2a) and (2b)] in three-dimensional space with coordinates

$$S^3 = (\theta,\dot{\theta},t) \tag{9}$$

is called a trajectory. A Poincaré map is constructed by projecting a selected sequence of points at discrete time $(\ldots, t_{i-1}, t_i, t_{i+1}, \ldots)$ from the trajectory onto the corresponding two-dimensional phase space:

$$S^2 = (\theta,\dot{\theta}). \tag{10}$$

For a periodically forced vibratory system, a Poincaré map may be obtained by sampling $(\theta,\dot{\theta},t)$ of the trajectory at the period of the forcing motion. For a periodic excitation T, periodic, quasi-periodic and chaotic responses may be defined in terms of the Poincaré map as follows:

(1) If the following two equations are satisfied

$$\theta(t+\alpha T) = \theta(t) \tag{11a}$$

$$\dot{\theta}(t+\alpha T) = \dot{\theta}(t) \tag{11b}$$

and α is bounded and rational, then the response is periodic. The corresponding Poincaré map consists of a finite number of fixed points. In particular, if $\alpha = p/q$, then the Poincaré map will contain exactly p fixed points.

(2) If α satisfies Equation (11a) and (11b), and is bounded but irrational, then the response is quasi-periodic. The corresponding Poincaré map will consist of an infinite number of points forming one or more closed curves. This may be considered as the extreme case where the irrational number α is approximated by two infinitely large, relatively prime numbers p and q, which form a finite quotient.

(3) If no bounded real number α exists that satisfies both Equation (11a) and (11b), then the response is called chaotic, and the corresponding Poincaré map is called a strange attractor.

The above mathematical definitions may be further interpreted in terms of iterated maps. If for example, $X_{n+1} = f(X_n)$ is a general map of n variables represented by the vector X, then a fixed point satisfies

$$X = f(X). \tag{12a}$$

The iteration of a map is often written $f(f(X)) = f^{(2)}(X)$ (Moon, 1987). Using this notation, an m-periodic orbit is a fixed point that repeats after m iterations of the map; that is

$$X_m = f^{(m)}(X_m) \tag{12b}$$

where m is the minimum integer satisfying Equation (12b). In practice, when the excitation is periodic with period T, a natural rule for a Poincaré map is to choose

$$t_n = NT + \tau_o \tag{13}$$

where τ_o is a time shift. It allows periodic and non-periodic responses to be distinguished. Let the (q,p) mode be the periodic response with period p/q time that of the excitation (Spanos and Koh, 1984). If the response is periodic, the points in the Poincaré map will converge to a finite number of fixed positions. Thus, harmonic, subharmonic and superharmonic responses appear on the map as equilibrium or fixed points. For instance, a (1,1) mode will converge to 1 point in a Poincaré map and a (1,3) mode converges to 3 points. When the response is quasi-periodic, the pattern on the Poincaré map presents several tori. When the response is chaotic, the Poincaré points generate a pattern called a *strange attractor* (Moon, 1987).

The Poincaré maps of one-third subharmonic, quasi-periodic and chaotic responses are shown in Fig. 8a–c, respectively. As expected, the three responses are shown to have three fixed point (periodic), closed curves (quasi-periodic), and a strange attractor (chaotic) which does not resemble fixed points or closed curves.

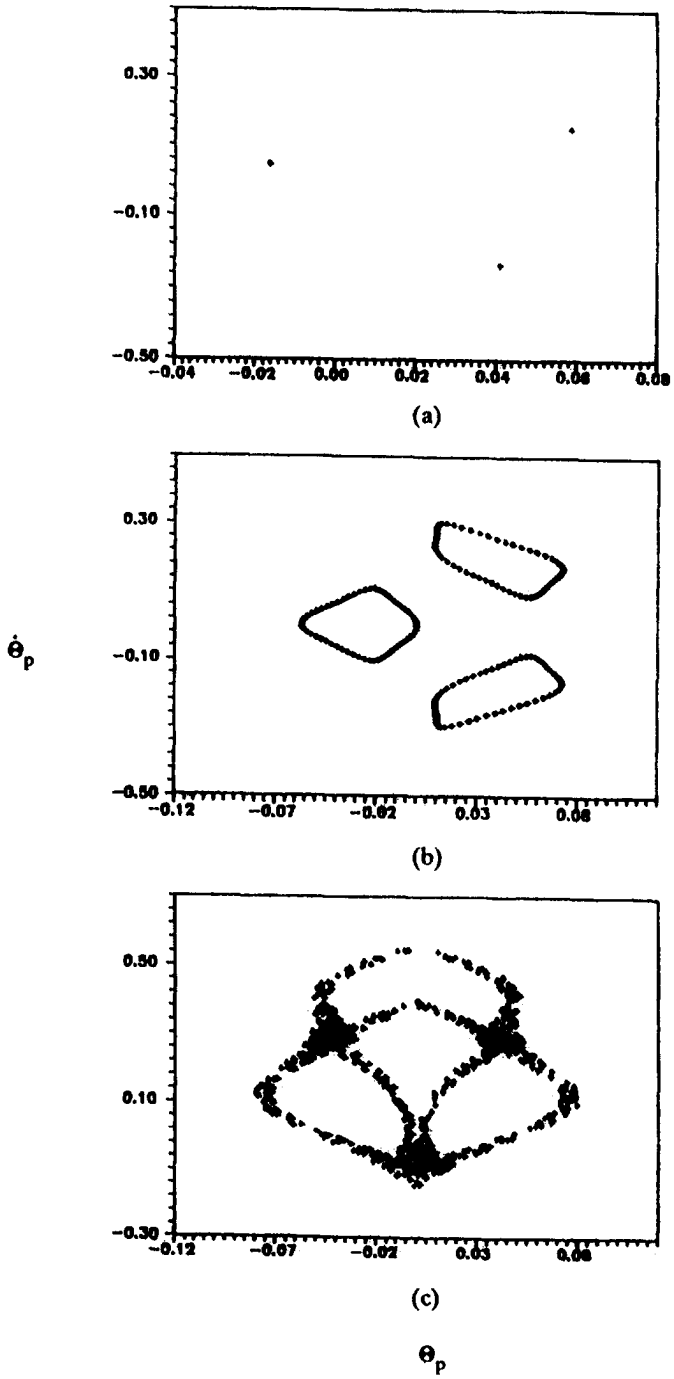

FIG. 8. Poincaré maps: (a) subharmonic response, $A_x = 6.5$, $T_x = 0.4$ and $e = 0.925$; (b) quasi-periodic response, $A_x = 4.0$, $T_x = 0.4$ and $e = 1.0$; (c) chaotic response, $A_x = 3.0$, $T_x = 0.4$ and $e = 1.0$.

4.2. *Verification techniques*

Two quantitative analysis techniques—Lyapunov exponent and fractal dimension—are employed to verify the types of responses in this study. These quantitative techniques are in general much more efficient and definitive indicators of chaotic response than the Poincaré map.

4.2.1. *Lyapunov exponent.* The Lyapunov exponent is a quantitative measure of the sensitivity of a system to initial conditions. It measures the average of exponential rates of divergence of nearby trajectories in phase space. Since nearby trajectories correspond to nearly identifical initial conditions, exponential orbital divergence means that systems with little initial difference (not resolvable within the accuracy of measurement) will soon behave quite differently leading to rapid loss of predictability. The Lyapunov exponent λ is defined by the equation

$$d = d_o 2^{\lambda(t-t_o)} \tag{14a}$$

where d and d_o denotes the distance between nearby trajectories at time t and the initial time t_o, respectively. For a given time history, the average of measurement (Moon, 1987) is expressed as

$$\lambda = \lim_{N\to\infty} \frac{1}{N} \sum_{1}^{N} \frac{1}{(t_i - t_{io})} \ln_2 \frac{d_1}{d_2}. \tag{14b}$$

The sign of a Lyapunov exponent provides a qualitative picture of a system's dynamics. One-dimensional systems are characterized by a single Lyapunov exponent which is positive for chaos, zero for quasi-periodic, and negative for a periodic orbit. In a three-dimensional continuous dissipative dynamical system the only possible spectra, and the attractors they describe, are as follows: (+,0,−), a strange attractor; (0,0,−), a two-torus; (0,−,−), a limit cycle; and (−,−,−), a fixed point.

In general, any system with bounded responses containing at least one positive Lyapunov exponent is defined to be chaotic, with the magnitude of the exponent reflecting the time scale on which system dynamics becomes unpredictable. In this study, a computer program is developed, based on Wolf *et al.* (1985), to calculate the Lyapunov exponents.

4.2.2. *Fractal dimension.* The property of a chaotic response in phase space can be characterized by the fractal dimension of its Poincaré map. A fractal dimension is a quantitative property of a set of points in an n-dimensional space which measures the extent to which the points fill a subspace. A set of points is said to be fractal if its dimension is non-integer—hence the term fractal dimension. A non-integer dimension is a hallmark of chaotic responses (Thompson and Stewart, 1987). A fundamental definition of the fractal dimension is derived from the notion of counting the number of spheres N of size ϵ needed to cover the orbit in phase space. Basically, $N(\epsilon)$ depends on the subspace of the orbit. If it is a periodic or limit cycle orbit then $N(\epsilon) \approx \epsilon^{-1}$. When the motion lies on a strange attractor, $N(\epsilon) \approx \epsilon^{-d}$. Taking the logarithms of the above statements (Moon, 1987), the fractal dimension can be expressed as:

$$d_c = \lim_{\epsilon \to 0} \frac{\log N(\epsilon)}{\log\left(\frac{1}{\epsilon}\right)}. \tag{15a}$$

Implicit in this definition is a requirement that the number of points in the set be large, i.e. $N \to \infty$. In this study, a computer program is developed based on Theiler (1987) to obtain the a form of fractal dimension of chaotic responses called the correlation dimension, which is given by:

$$d_c = \lim_{r \to 0} \lim_{N \to \infty} \frac{\log C(N,r)}{\log r} \tag{15b}$$

where $C(N,r)$ is the correlation integral, which can be numerically evaluated as follows [Theiler (1987) and Moon (1987)]:

$$C(N,r) = \frac{\text{No. of distance less than } r}{\text{No. of distance altogether}} \tag{15c}$$

5. RESPONSE BEHAVIOR

The characteristics of the response behavior of free-standing rocking objects are studied in detail using the analytical and numerical techniques developed above. The time-histories, phase diagrams, Poincaré maps, Lyapunov exponents and fractal dimensions of the responses are computed. The responses of the simplest possible system (undamped and slender), whose only nonlinearity results from transition of the governing equation of motion, is first examined to establish the elements rocking behavior. The results serve as a baseline reference for determining the influence of other nonlinear effects. Parametic maps are employed to determine the influence of the other three nonlinearities—energy dissipation, geometry and parametric excitation, on the rocking behavior. The frequency of occurrence of chaotic response is used as an indicator of the sensitivity of the response.

5.1. *Response characteristics of undamped systems*

The intrinsic characteristics of rocking response, which is caused by the nonlinearity due to the transition of governing equations of motion alone, can be determined by examining the *simplest* (undamped and slender) rocking system. This system assumes that: (1) the energy dissipation at impact is negligible so that the coefficient of restitution, e, is unity; (2) the rigid object is slender so that the response is independent of the slenderness ratio; and (3) the vertical excitation is identically zero so that there is no nonlinear coupling between excitation and response. Under these assumptions, the responses are found to be either *quasi-periodic*, *chaotic* or *overturning*; no periodic response exists.

Typical time-histories and phase-diagrams of quasi-periodic and chaotic responses of an undamped system are shown in Figs 4 and 5, respectively. As mentioned earlier, the time-histories and phase-diagrams of the two types of responses are rather similar. However, the Poincaré maps of the quasi-periodic response (Fig. 8b) clearly exhibit the characteristics of tori. The Poincaré map of the chaotic response (Fig. 8c) also exhibits the characteristics of a *strange attractor*. The classification of the two types of

responses are further confirmed by their Lyapunov exponents and the fractal dimensions, which are 0.0 and 2.0, respectively, for the quasi-periodic response, and 0.14 and 2.3, respectively, for the chaotic response.

A parametric map of the response of the simplest system to horizontal excitation alone, varying period and amplitude of the horizontal excitation (with quiescent initial conditions), is shown in Fig. 9. As stated above, only quasi-periodic and chaotic responses are found to co-exist with overturning response. Thus it can be claimed that the rocking responses of undamped systems are characterized by their sensitivity to initial conditions and system and excitation parameters.

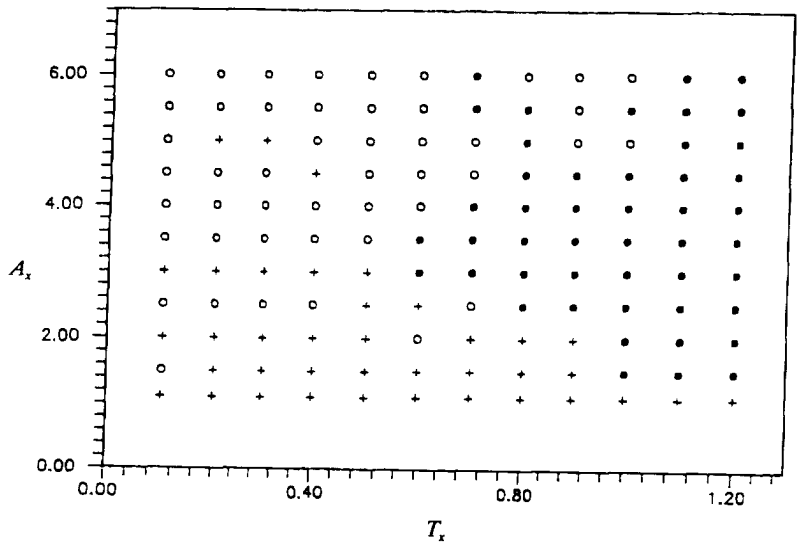

FIG. 9. Parametric map of undamped slender systems: chaotic response +, quasi-periodic response ○, and overturning response •; $R = 290$, $H/B = 10$ and $e = 1.0$.

5.2. *Response characteristics of damped systems*

The effects of energy dissipation (nonlinear damping) at impact on the response behavior of the rocking system can be determined by examining the behavior of systems with coefficient of restitution, e, less than unity. Damped systems eliminate assumption (1), but still retain the large slenderness ratio, and no vertical excitation assumptions [assumptions (2) and (3)]. Under these assumptions, with quiescent initial conditions, the responses are found to be either periodic or overturning. Typical time-histories and phase-diagrams of an overturning response and a one-third subharmonic response were shown in Figs 3 and 4, respectively. The Poincaré maps of the periodic response (Fig. 8a) show the fixed points at one-third that of the excitation. The Lyapunov exponents and the fractal dimensions are 0.0 and 0.0, respectively, which confirm the periodic nature of the response.

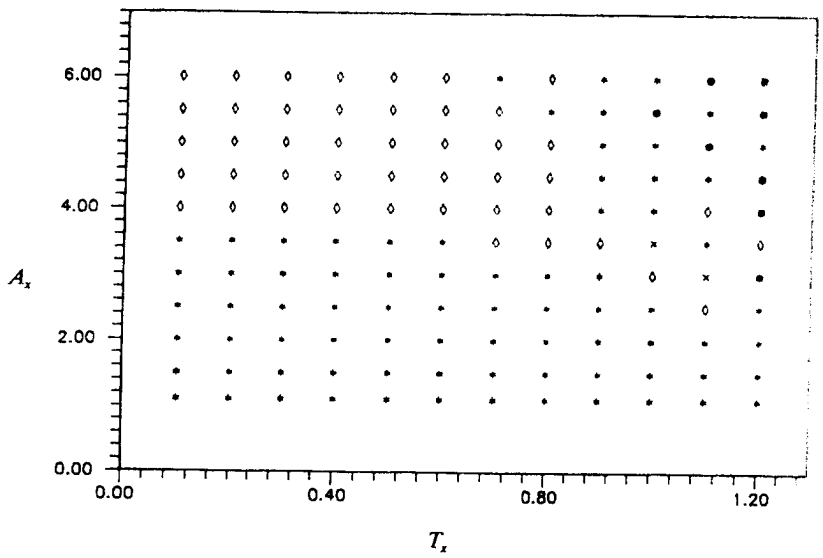

FIG. 10. Parametric map of damped slender systems: harmonic response *, one-third subharmonic response ◊ and overturning response •; $R = 290$, $H/B = 10$ and $e = 0.95$.

A parametric map of the responses of damped systems, varying period and amplitude of the horizontal excitation, is shown in Fig. 10. As indicated, only periodic responses are found to co-exist with overturning response. No quasi-periodic or chaotic responses are found. This observation is confirmed by an extensive numerical search over a wide range of system and excitation parameters. Because periodic responses are relatively more stable than quasi-periodic and chaotic responses, it can be stated that the responses of damped systems are characterized by their stability with respect to small perturbation in initial conditions and system parameters.

5.3. *Effects of slenderness ratio*

For systems with large slenderness ratios, previous studies (Yim *et al.*, 1980) indicated there is good agreement between analytical predictions from the linearized system and the numerical results obtained from the fully nonlinear system. However, large differences between linearized and fully nonlinear systems may result if the slenderness ratio is small.

As shown in the response time history (Fig. 11), the slenderness ratio (geometric nonlinearity) affects not only the amplitude but also the order of the response mode. As the slenderness ratio decreases from 4 to 1, the response amplitude decreases. In addition, the mode changes from (1,1) for $H/B = 4$ to (1,3) for $H/B = 2$ and back to (1,1) for $H/B = 0.4$. The parametric maps (Fig. 12a,b) show that systems with small aspect ratios are harder to set into rocking than systems with large aspect ratios, and various modes can be generated by varying aspect ratios. Furthermore, decreasing the aspect ratio decreases the region of overturning. In other words, the stability of the rocking response of an object subjected to external excitation increases with decreasing

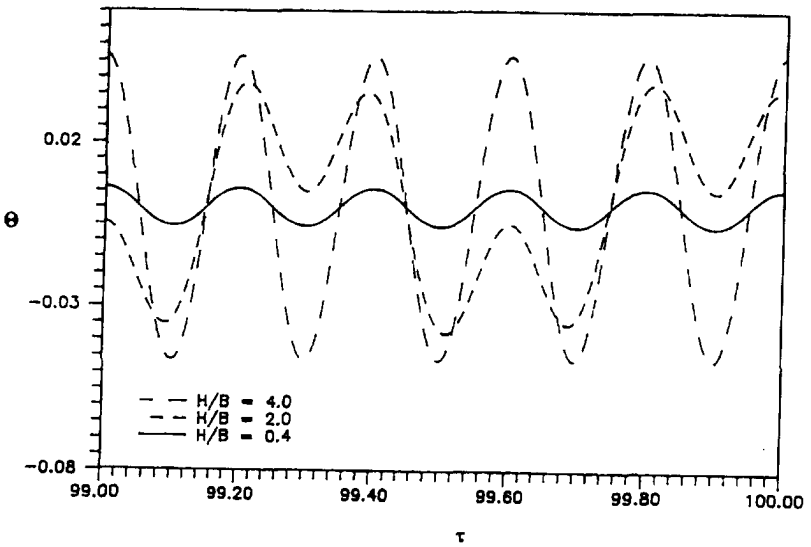

FIG. 11. Effects of geometric nonlinearity on rocking responses: time history; $a_x = 0.3$, $T_x = 0.2$ and $e = 0.925$.

slenderness ratio. Based on extensive numerical results examined, systems with a slenderness ratio of 5 and higher may be considered "slender". For these slenderness ratios, piecewise-linear equations will provide sufficiently accurate results in general.

5.4. *Effects of vertical excitation*

The analyses and observations presented in the above sections are for systems subjected to horizontal excitation only. However, in many practical situations, especially in the offshore environment, the vertical component of the excitation often cannot be neglected. Thus it is essential to examine the influence of the vertical excitation on the behavior of the rocking response.

The effects of vertical excitations are examined here for both undamped and damped rocking systems. In each case, the parametric maps for responses with and without vertical excitations are compared. In addition, the effects of frequency and amplitude ratios (between vertical and horizontal excitations) are also examined.

5.4.1. *Undamped slender systems.* To determine the influence of vertical excitation on the response behavior of undamped systems, parametric maps of systems subjected to horizontal excitation only, and the corresponding systems subjected to both horizontal and vertical excitations, are examined (Fig. 13a,b). The maps consist of responses to varying amplitudes and frequencies of horizontal excitations. The vertical-to-horizontal excitation amplitude ratio r_a is held at 0.5, while the excitation frequencies are identical. For both cases, the only responses observed are quasi-periodic, chaotic and overturning. No stable periodic response exists. The parametric maps indicate that much more overturning occurs for the systems subjected to horizontal and vertical excitations than

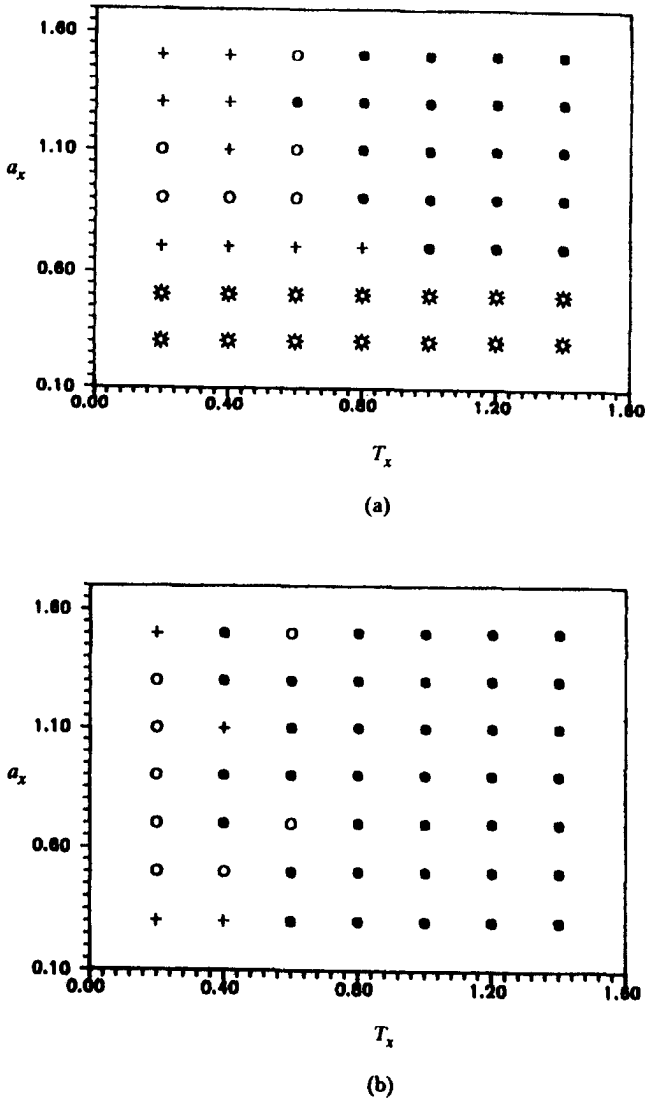

FIG. 12. Effects of geometric nonlinearity on rocking responses: parametric maps; (a) $H/B = 2$, (b) $H/B = 10$; chaotic response +, quasi-periodic response ○, overturning response ●, and no rocking response ✲; $R = 120$ and $e = 1.0$.

those subjected to horizontal excitation alone. Thus vertical excitation reduces the overturning stability of the system. The maps also show that the presence of vertical excitation can change the resulting response types (and hence characteristics), from quasi-periodic to chaotic and vice versa, in a rather random fashion. There does not appear to be a describable pattern in how the responses are affected.

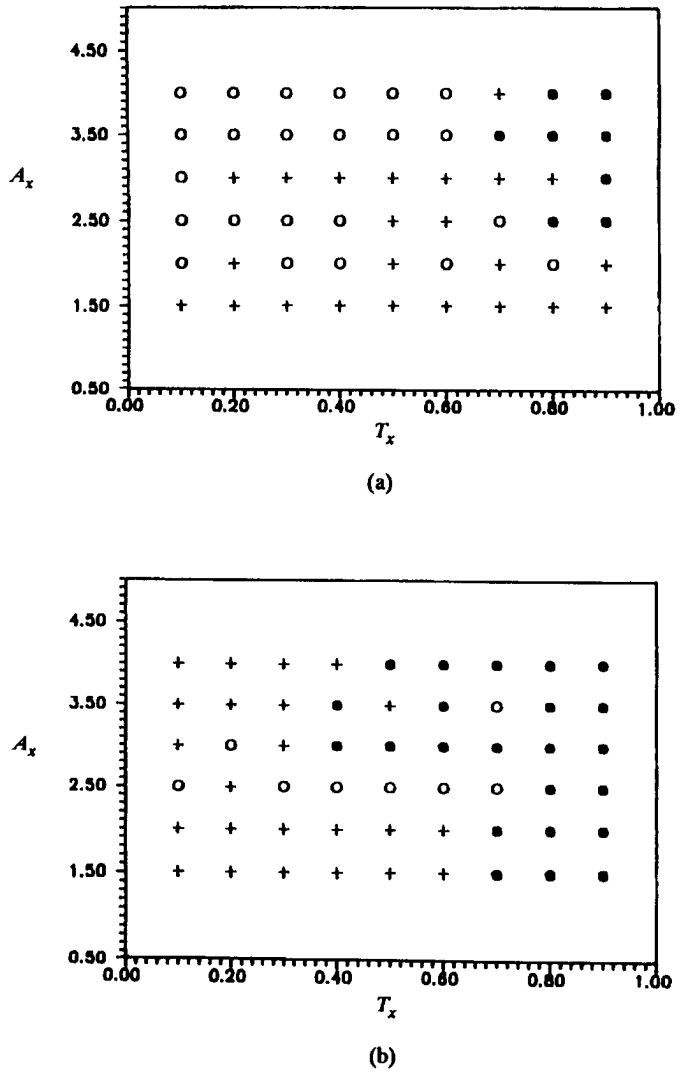

FIG. 13. Effects of vertical excitation on undamped rocking systems (e = 1): (a) slender system subjected to horizontal excitation only, and (b) slender system subjected to horizontal and vertical excitation with r_a = 0.5 and r_f = 1.0; chaotic response +, quasi-periodic response ○, overturning response •.

5.4.2. *Damped systems*

5.4.2.1. *Damped slender systems.* The presence of vertical excitation induces some unexpected response characteristics to the damped systems. As shown in Fig. 14a, for the damped system subjected to only horizontal excitation, the stable responses consist of only symmetric (1,1) modes and (1,3) modes. The boundary between these modes

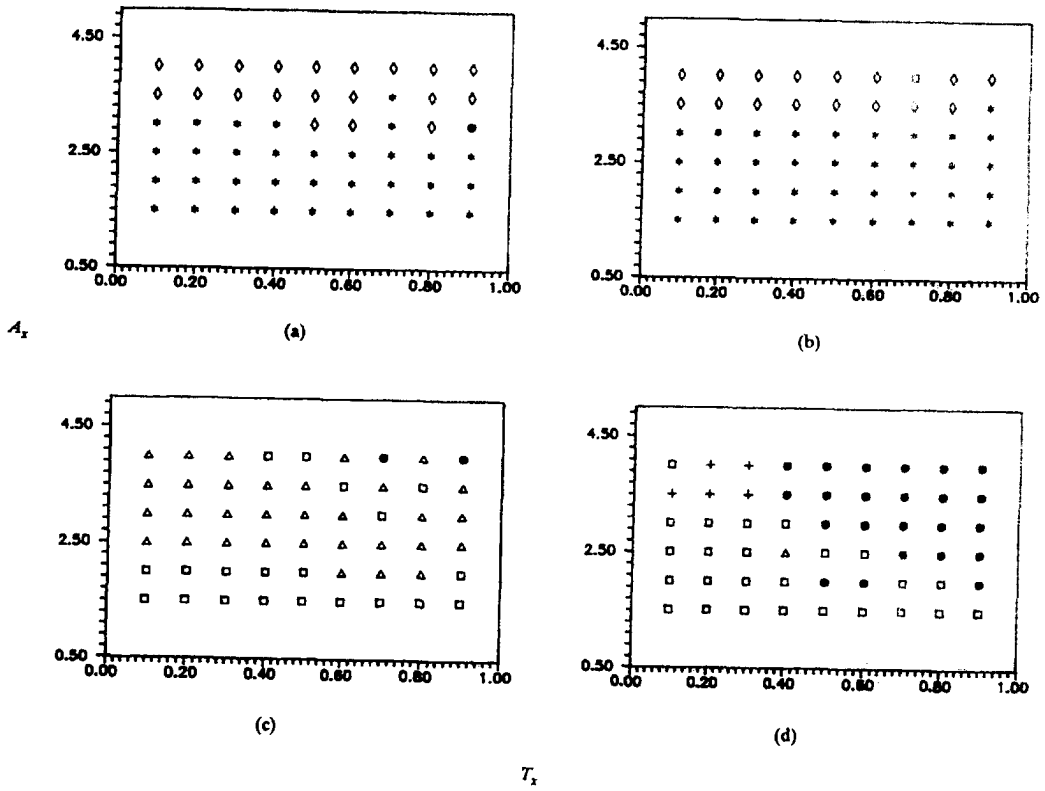

FIG. 14. Effects of vertical excitation on slightly damped rocking systems (e = 0.98): (a) slender system subjected to horizontal excitation only (H/B = 10), (b) slender system subjected to horizontal and vertical excitation (H/B = 10), (c) rocking system with finite slenderness subjected to horizontal excitation (H/B = 2), (d) rocking system with finite slenderness ratio subjected to horizontal and vertical excitations (H/B = 2); chaotic response +, quasi-periodic response ○, overturning response ●, harmonic response *, one-third subharmonic response ◊, even-order subharmonic response □, and odd-order subharmonic response Δ; R = 290

and overturning response are smooth. However, when vertical excitation is present (Fig. 14b), the response behavior becomes much more complex. First, when the vertical excitation amplitude is relatively large, a number of odd modes become unsymmetric. Second, unsymmetric even modes, which do not exist when vertical excitation is absent, become dominant modes of response. Third, the boundaries of each type of response become scattered. The added complexity of the periodic responses and the frequent, irregular transitions between different types of responses indicate that the system is more sensitive with the presence of vertical excitation.

5.4.2.2. *Damped systems with finite slenderness ratio.* The parametric maps of a damped system with finite slenderness ratio subjected to horizontal excitation only, and to both horizontal and vertical excitations, are shown in Fig. 14c and d, respectively. The responses of the system with only horizontal excitation are symmetric odd periodic modes. No chaotic response is observed. However, when vertical excitation is present,

as in the slender case, the parametric map becomes significantly more complex. Chaotic response, unsymmetric odd and even modes and overturning responses are observed. The number of symmetric responses are significantly reduced, and unsymmetric periodic modes become dominant. Furthermore, transitions between different unsymmetric modes and chaotic response occur frequently. It may be concluded that the presence of vertical excitation increases the sensitivity of the response significantly in rocking systems with finite slenderness ratio.

5.4.3. *Effects of frequency and amplitude ratios*

To examine the effects of varying vertical excitation frequency and amplitude ratios on rocking response, the parametric maps of an undamped ($e = 1$), a slightly damped ($e = 0.98$), and a damped system ($e = 0.9$) are presented in Fig. 15a–c, respectively. In these figures, the vertical-to-horizontal amplitude and frequency ratios (ordinate and abscissa, respectively) are varied, while the amplitude and frequency of the horizontal excitation are held fixed. It is observed that the characteristics of the responses can be significantly influenced by varying the vertical frequency and amplitude ratios in all three cases.

For the undamped system (Fig. 15a), a large vertical excitation amplitude leads to overturning response. As the amplitude ratio decreases, (bounded) chaotic response becomes prevalent. For low values of amplitude ratio, quasi-periodic responses become predominant. These effects are consistent with that of varying horizontal excitation amplitude alone. Varying the frequency of the vertical excitation can also change the characteristics of the response for a wide range of vertical excitation amplitude ratios around 0.4.

As expected, when damping ($e = 0.98$) is introduced, albeit very small in magnitude, the region of chaotic response decreases (Fig. 15b). Quasi-periodic responses completely disappear and periodic responses become dominant, and the periodic responses are much more complex than those induced by horizontal excitation alone. The parametric map clearly demonstrates that although the parameters of the horizontal excitations are fixed, by varying the amplitude and frequency ratios, the characteristics of the response can change from overturning to chaotic, and various subharmonics.

When damping is further increased, the regions of overturning responses disappear (Fig. 15c). However, chaotic responses still exist among various types of subharmonic responses, although less extensively. Even-order periodic responses continue to dominate. These observations indicate that parametric excitation (the coupling of vertical excitation with rocking motion) has a strong influence on the sensitivity of rocking response.

6. CONCLUSIONS

The response behavior of free-standing equipment in the offshore environment is found to be much more complex than that examined in previous studies of rocking systems. Chaotic and quasi-periodic responses are discovered in this study. It is demonstrated that the major cause of sensitivity of the rocking is due to the transition of governing equations at impact. For undamped systems, it induces quasi-periodic and chaotic responses.

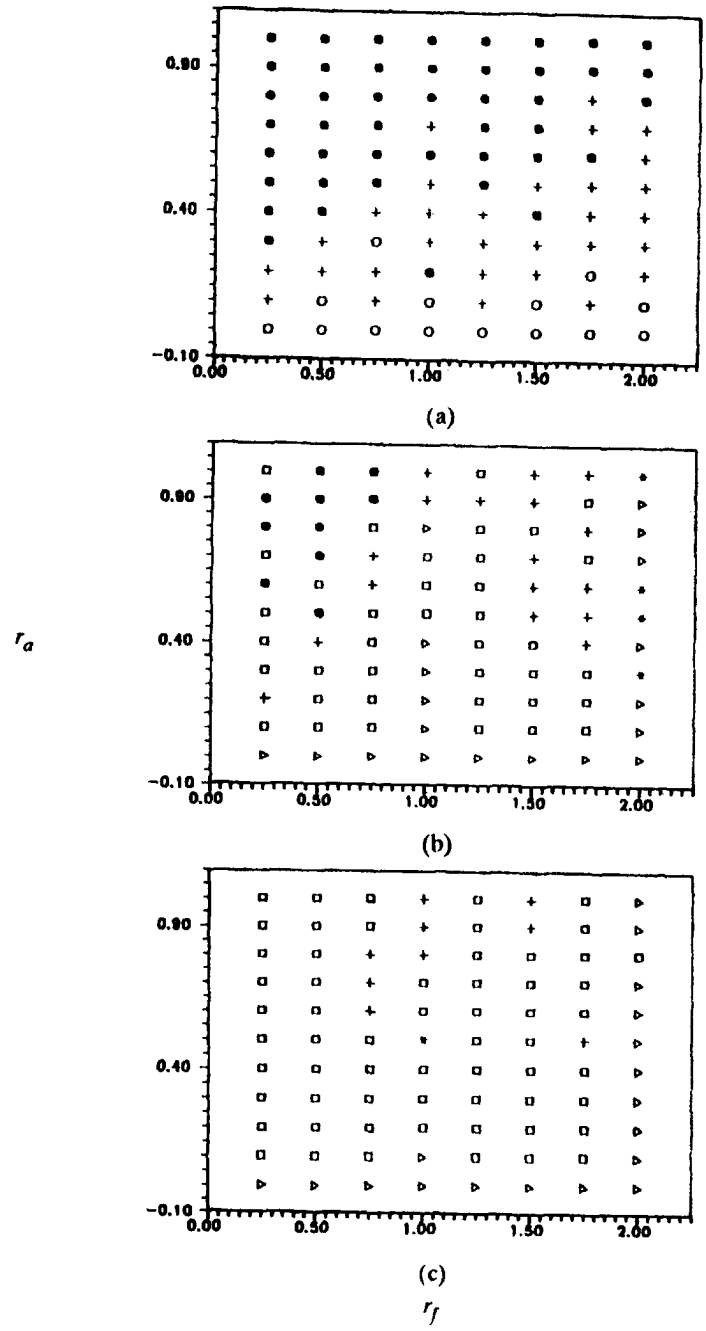

FIG. 15. Effects of vertical excitation amplitude and frequency ratios on the rocking systems with finite slenderness ratio: (a) undamped system, (b) slightly damped system ($e = 0.98$), and (c) damped system ($e = 0.9$); chaotic response +, quasi-periodic response ○, overturning response •, harmonic response ∗, odd-order subharmonic response ▷, and even-order subharmonic response □; $R = 290$, $H/B = 4$, $A_r = 4$ and $T_r = 0.3$.

On the other hand energy dissipation has a stabilizing effect on the responses. In fact, based on numerical results, with quiescent initial conditions, quasi-periodic and chaotic responses do not occur for systems subjected to horizontal excitation alone when damping is present. Thus, damping lowers the level of sensitivity of a rocking system.

When the system is subjected to horizontal excitation alone, geometric nonlinearity (finite slenderness ratio) also has a stabilizing effect, although its influence is not as significant as energy dissipation. It is observed that the smaller the slenderness ratio of the object, the more stable the rocking response becomes. In general, the rocking response is more likely to contain higher modes (and in the limit quasi-periodic and chaotic responses) when the system has a large slenderness ratio, and a coefficient of restitution close to unity.

The influence of vertical excitation is rather significant, and not systematic. In general, vertical excitation increases the sensitivity of the rocking response. The parametric maps of the systems subjected to both vertical and horizontal excitations are much more complex than those of the systems subjected to horizontal excitation only. Chaotic response occurs much more frequently. Because the symmetry of the system is destroyed when vertical excitation is present, the unsymmetric even modes become dominant compared with the symmetric odd modes. With vertical excitation, the effect of geometric nonlinearity is much less systematic. Contrary to the case of no vertical excitation, chaotic response appears more often with smaller slenderness ratio when vertical excitation is present.

For systems subjected to horizontal excitation only, damping tends to stabilize the system response by reducing the region of chaotic response and shortening the duration of transient motion. However, for systems with vertical excitation, the effect of damping is less systematic. Chaotic response can occur in the case with large damping. The transient responses do not always reduce monotonically with increasing damping.

This study has clearly demonstrated that, for some combinations of system and excitation parameters, the rocking response can become extremely sensitive to even the simplest form of excitations—periodic excitation. Furthermore, the presence of vertical excitation increases the complexity and sensitivity of the response behavior. Thus it is not surprising that rocking response can be extremely sensitive to complex, random earthquake excitations, where vertical excitation is significant, as illustrated by the shaking table experiments (Aslam *et al.*, 1980). The unidentified complex responses observed in dynamic rocking object tests by Wong and Tso (1989) may be the quasi-periodic or chaotic responses discovered in this study. Since the motions of the supporting base of free-standing offshore equipment are induced by random waves and currents, similar degrees of sensitivity of the rocking response can be expected.

Acknowledgement—The authors gratefully acknowledge the financial support for this research by the Office of Naval Research Young-Investigator Award under grant No. N00014-88-K-0729.

REFERENCES

ASLAM, M., GODDEN, W.G. and SCALISE, D.T. 1980. Earthquake rocking response of rigid bodies. *J. Struct. Engng Div., ASCE* **106**, 377–392.

HOUSNER, G.W. 1963. The behavior of inverted pendulum structures during earthquakes. *Bull. seism. Soc. Am.* **53**, 403–417.

ISHIYAMA, Y. 1982. Motion of rigid bodies and criteria for overturning by earthquake excitations. *Earthquake Engng Struct. Dynamics* **10**, 635–650.

MOON, F.C. 1987. *Chaotic Vibrations*. Wiley and Sons, New York.

NAYFEH, A.H. and MOOK, D.T. 1979. *Nonlinear Oscillations*. Wiley and Sons, New York.

SPANOS, P.D. and KOH, A.S. 1984. Rocking of rigid blocks due to harmonic shaking. *J. Engng Mech. Div., ASCE* **110**, 1627–1642.

THEILER, J. 1980. Efficient algorithm for estimating the correlation dimension from a set of discrete points. *Physica Rev. A* **36**, 4456–4462

THOMPSON, J.M.T. and STEWART, H.B. 1986. *Nonlinear Dynamics and Chaos*. Wiley and Sons, New York.

TSO, W.K. and WONG, C.M. 1989. Steady state rocking response of rigid blocks, Part I: analysis. *Earthquake Engng Struct. Dynamics* **18**, 89–106.

WOLF, A., SWIFT, J.B., SWINNEY, H.L. and VASTANO, J.A. 1985. Determining Lyapunov exponent from a time series. *Physica 16D* **16**, 285–317.

WONG, C.M. and TSO, W.K. 1989. Steady state rocking response of rigid blocks, Part II: experiments. *Earthquake Engng Struct. Dynamics* **18**, 107–120.

YIM, C.S., CHOPRA, A.K. and PENZIEN, J. 1980. Rocking response of rigid blocks to earthquakes. *Earthquake Engng Struct. Dynamics* **8**, 565–587.